

## An on-line infrared spectroscopic system with a modified multipath White cell for direct measurements of N<sub>2</sub>O from NH<sub>3</sub>-SCR reaction

Dong Woo Kim\*, Moon Hyeon Kim\*<sup>†</sup>, and Sung-Won Ham\*\*

\*Department of Environmental Engineering, Daegu University, 15 Naeri, Jillyang, Gyeongsan 712-714, Korea

\*\*Department of Display and Chemical Engineering, Kyungil University, 33 Buho, Hayang, Gyeongsan 712-701, Korea

(Received 30 January 2010 • accepted 15 March 2010)

**Abstract**—An on-line, continuous IR-based N<sub>2</sub>O measurement system has been developed by combining with a variable multipath “White cell” to avoid a huge amount of the well-known artifact errors in actual N<sub>2</sub>O concentrations determination when analyzing grab samples taken from stationary sources, such as fossil fuel-fired power plants. For solving the problems confronted in earlier stages of this study, the gas cell had to have modifications of the feed through of gas sample flows, the multilayer coatings of stainless steel mirrors, and the thermal efficiency to provide high cell inner temperatures in flowing gas samples. These modifications allow good tolerance of the gas cell to gases and chemicals, such as NO<sub>x</sub> and NH<sub>3</sub>, and NH<sub>4</sub>NO<sub>3</sub> driven from them, and its usage for a long lifetime even under harsh conditions. They also offer excellent performance not only in directly determining the extent of N<sub>2</sub>O formation during the course of NH<sub>3</sub>-SCR reaction over a sample of a commercial V<sub>2</sub>O<sub>5</sub>-WO<sub>3</sub>/TiO<sub>2</sub> catalyst, but also in simultaneously monitoring changes in concentrations of NO, NO<sub>2</sub> and NH<sub>3</sub> during the reaction. Each reference peak was chosen in gas-phase spectra for N<sub>2</sub>O, NO<sub>x</sub>, NH<sub>3</sub> and H<sub>2</sub>O, and CO<sub>2</sub> as a possible interference, and the modified gas cell was finely tuned to obtain their spectra with a high resolution under optimal operating conditions. The catalyst gave significant amounts of N<sub>2</sub>O formation at reaction temperatures greater than 350 °C, and attention should be paid to the possibility of N<sub>2</sub>O production from commercial NH<sub>3</sub>-SCR deNO<sub>x</sub> processes with V<sub>2</sub>O<sub>5</sub>/TiO<sub>2</sub>-based catalysts.

Key words: Long Path White Cell, On-line N<sub>2</sub>O Measurements, Commercial V<sub>2</sub>O<sub>5</sub>-WO<sub>3</sub>/TiO<sub>2</sub> Catalysts, NH<sub>3</sub>-SCR Reaction, N<sub>2</sub>O Formation

### INTRODUCTION

Nitrous oxide (N<sub>2</sub>O) possesses a much greater global warming potential (GWP), by 310 times over a 100-year time horizon, than does CO<sub>2</sub>, and it has approximately a 150 year lifetime in the atmosphere [1,2]. Anthropogenic sources such as adipic acid production, circulating fluidized bed combustions, nitric acid synthesis and the use of anesthetic in medical operating rooms of hospitals occupy large amounts in N<sub>2</sub>O emissions, except for its predominant emissions from natural sources by microbial action in soils and oceans [2-5]. Recently, commercial processes that are operating at fossil fuel-fired power plants to eliminate NO<sub>x</sub> are suspiciously likely to be another anthropogenic source of N<sub>2</sub>O emissions, because numerous V<sub>2</sub>O<sub>5</sub>/TiO<sub>2</sub>-based catalysts being widely used for such deNO<sub>x</sub> processes have been reported to produce N<sub>2</sub>O with concentrations ranging from 20 to 800 ppm during the selective catalytic reduction (SCR) of NO<sub>x</sub> by NH<sub>3</sub> in the presence of O<sub>2</sub> [3,6-13], designated to “NH<sub>3</sub>-SCR”, although the extent of the formation of N<sub>2</sub>O during NH<sub>3</sub>-SCR reaction depended strongly on a variety of catalyst features and operating parameters, such as the kind of catalysts and their compositions, the kind of supports and their physicochemical properties, the reaction temperature, and the ratio between gases fed. These previous works suggest that the widespread use of the conventional SCR catalysts can affect the global warming, when considering the high GWP value of N<sub>2</sub>O.

Stationary combustion of fossil fuels was reported to be a significant source of atmospheric N<sub>2</sub>O emissions in a previous investigation [14] in which the production of N<sub>2</sub>O exceeding 100 ppm was observed during their combustion in a large experimental combustor, and another fundamental study on coal combustion claimed that fuel nitrogen present in coals might be converted to form huge amounts of N<sub>2</sub>O [15]. However, all these works were argued because an artifact during a sampling to measure actual concentrations of N<sub>2</sub>O existing in flue gases from the combustion sources was proposed [16,17]. The artifact would be created by the use of a grab sampling and then when allowing the samples to be awaiting for determining N<sub>2</sub>O concentrations, thereby giving substantial N<sub>2</sub>O formation in sample containers, as clearly verified by an experimental observation that large amounts of N<sub>2</sub>O could be produced when a gas mixture containing both NO<sub>x</sub> and SO<sub>2</sub> with high concentrations of thousands of ppms was passed through a weak sulfuric acid solution vessel [18], although N<sub>2</sub>O formation levels depended strongly not only on the SO<sub>2</sub> concentrations, but also on whether or not the both gases were contacted for a sufficient time. To prevent such artifact errors in grab sample measurements, the use of on-line instruments, representatively infrared (IR) spectroscopy and gas chromatography coupled with proper detection devices, for direct N<sub>2</sub>O measurements exhibited less than 5 ppm of N<sub>2</sub>O emissions even from full-scale utility boilers [18,19], which is in excellent agreement with studies of the extent of N<sub>2</sub>O formation for the combustion of fossil fuels in power plants [20]. This emission level is widely accepted to be a peak concentration observable at the fossil fuels-fired power plants without NH<sub>3</sub>-SCR deNO<sub>x</sub> processes.

<sup>†</sup>To whom correspondence should be addressed.  
E-mail: moonkim@daegu.ac.kr

Based on the early studies which reported the formation of N<sub>2</sub>O with huge amounts in NH<sub>3</sub>-SCR reaction with V<sub>2</sub>O<sub>5</sub>/TiO<sub>2</sub>-based catalysts and the secondary N<sub>2</sub>O formation during transport and storage of grab samples [3,6-13,16-18], an on-line analysis system with a very fast response is required to directly measure N<sub>2</sub>O concentrations produced from NH<sub>3</sub>-SCR reaction. This is one of the best ways of avoiding such artifacts in determining actual N<sub>2</sub>O emissions. Therefore, the present study has focused on how to configure an on-line IR analysis system combined with a modified "White cell" for allowing direct, continuous measurements of N<sub>2</sub>O from commercial NH<sub>3</sub>-SCR processes. For this purpose, we describe some requirements for a successful N<sub>2</sub>O measurement system that will be the minimum purity of gases used for a laboratory model NH<sub>3</sub>-SCR reaction to differentiate N<sub>2</sub>O present in fossil fuels-fired power plants, the necessary components and modifications of the gas cell to operate it at high temperatures and in a flow of harsh gases, and the reasonable vehicles to solve and/or prevent physical contaminations and chemical alteration of the surface of mirrors in the gas cell. Finally, this well-configured system coupled with such a modified White cell was used to directly determine the extent of N<sub>2</sub>O production for NH<sub>3</sub>-SCR reaction with a commercial V<sub>2</sub>O<sub>5</sub>-WO<sub>3</sub>/TiO<sub>2</sub> catalyst.

## EXPERIMENTAL

### 1. Catalyst

A fresh sample of a honeycomb-type commercial V<sub>2</sub>O<sub>5</sub>-WO<sub>3</sub>/TiO<sub>2</sub> catalyst was provided from a domestic coal-fired power plant, and it was crushed and gently ground to powder, prior to being used to investigate the extent of the formation of N<sub>2</sub>O during NH<sub>3</sub>-SCR reaction under given conditions. The physicochemical properties of the powder sample used here are listed in Table 1; however, no details in chemical compositions of this SCR catalyst except for V<sub>2</sub>O<sub>5</sub> and WO<sub>3</sub> can be provided here, because of a secrecy agreement with the catalyst supplier.

### 2. Ppm Levels of Impurities in Pure Gases

Ultrahigh purity N<sub>2</sub>O (Scott Specialty Gases Inc., VLSI grade, 99.999%), NH<sub>3</sub> (Scott Specialty Gases Inc., Electronic grade, 99.999%) and NO (Scott Specialty Gases Inc., Omega grade, 99.99%) with an aluminum cylinder were employed here, but the level of impu-

rities present in each cylinder was determined at the Specialty Gases Analysis Center, Scott Specialty Gases, USA as a unit of ppm to acquire possible interferences to direct N<sub>2</sub>O measurements. The N<sub>2</sub>O contained less than 1.5 ppm for all IR-active impurities being of interest here, as listed in Table 2. The respective pure NO and NH<sub>3</sub>

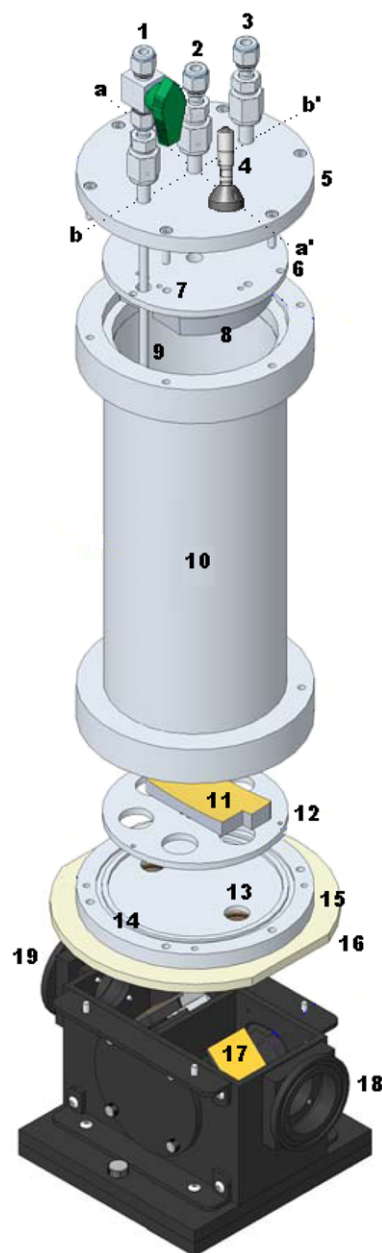


Fig. 1. Components of a variable long path White cell: 1, sample inlet port; 2, port for thermocouple insertion and pressure gauge connection; 3, sample outlet port; 4, pathlength adjustment micrometer; 5, valve and fitting endplate; 6, precision objective mirror fixing tray; 7, optical alignment adjuster; 8, multilayer-coated objective mirror; 9, sample feed-through tube; 10, cell body; 11, multilayer-coated field mirror; 12, precision field mirror nesting tray; 13, ZnSe window; 14, O-ring for vacuum and pressure seals; 15, window fixing endplate; 16, ceramic insulating endplate; 17, plane Au-coated transfer mirror; 18, beam inlet KBr window; 19, beam outlet KBr window.

Table 1. Physicochemical properties of a commercial SCR catalyst

Catalyst	Amount (%)		$S_{BET}$ (m <sup>2</sup> /g)	Mean pore diameter (nm)
	V <sub>2</sub> O <sub>5</sub>	WO <sub>3</sub>		
V <sub>2</sub> O <sub>5</sub> -WO <sub>3</sub> /TiO <sub>2</sub>	1.68	7.6	73	13.8

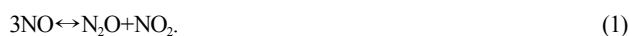
Table 2. Impurities levels of gases used

Gas	Purity (%)	Impurity (ppm)						
		N <sub>2</sub> O	NO <sub>2</sub>	N <sub>2</sub>	O <sub>2</sub>	THC <sup>a</sup>	CO <sub>2</sub>	H <sub>2</sub> O
N <sub>2</sub> O	99.999	-	0.1	1.2	0.4	0.01	0.3	0.7
NO	99.99	10.3	10.7	8.6	0.2	0.13	0.3	0.2
NH <sub>3</sub>	99.999	1.3	-	2.8	1.1	0.30	0.6	1.4

Note. "-"=no data or not applicable; THC=total hydrocarbons

<sup>a</sup>As CH<sub>4</sub>

had 8.6 and 2.8 ppm  $N_2$ , but this molecule is IR-inactive. The pure NO gas included 10.3 ppm  $N_2O$  and 10.7 ppm  $NO_2$  as impurities, which is due to auto-oxidation reaction between NO gases at high cylinder pressures, according to the following stoichiometry:



This  $N_2O$  impurity level will become about 5 ppb  $N_2O$  if a flowing mixture of pure He (Praxair, 99.999%) with 500 ppm NO at a total flow rate of 1,000  $cm^3/min$  is used, and it is under detection limits of our  $N_2O$  measurement system that will be described below.

### 3. Components and Geometry of a Variable Long Path White Cell and Its Modifications

#### 3-1. Major Components of the White Cell

A pathlength-adjustable gas cell (Zemini Scientific Instr., Model MARS 0.75L/8.0V) with a 0.75-L internal volume was used to directly measure  $N_2O$  emission levels during  $NH_3$ -SCR de $NO_x$  reaction with the commercial SCR catalyst, but this gas cell requires some modifications as discussed below. The physical design and the components of the gas cell are schematically shown in Fig. 1, which is a common cell design for gas analysis applications. Among a variety of the components consisting of the gas cell, optical mirrors are a critical component to define the line-up of the infrared images and the pass numbers of an IR beam entered into the White cell. Two objective mirrors-8 (shown for only a right one), hereafter numbers next to the dash are of indication of each component marked in Fig. 1, were placed onto a compound angular plate on each corresponding platform (not shown here) that is held on a mounting tray-6, and the alignment of these mirrors determines the cell pathlength that is ideally adjustable from 1.2 to 10 m by using a micrometer feedthrough adjustor-4 coupled with an optical alignment adjustor-7. The field mirror-11 was permanently fixed on a nesting tray-12. These two kinds of the mirrors were fabricated using a stainless steel (SS) and electropolished before a consecutive coating of suitable reflective materials. The SS mirrors require multi-layer coatings of Ni and Au, leading to very expensive mirrors, in which the Ni base coating was to protect the SS substrate of the mirrors even under harsh conditions including  $NO_x$ ,  $NH_3$  and  $SO_2$ , thereby allowing excellent chemical tolerance to such gases, and the Au was used for a primary reflective surface coating. The lifespan of the reflective coatings on mirrors is strongly associated with coating compositions, and gases to which the surface of the coated mirrors is exposed.

Line connections that are to allow a flow of samples entering and exiting the gas cell were made with commercially available 1/4" valves and fittings-1, 2 and 3, which are carried by using an end-plate-5, and these are easily detachable from a cylindrical main body-10 without affecting the other cell components and optical alignment. The cell body was fabricated with an SS material accompanying Ni coatings on the inner surface with electropolishing, and it was able to heat to 200 °C using a BriskHeat BS0 Series heating tape which had been connected to a Digi-Sense R/S PID temperature controller (Eutech Instr.). Although the outer surface of the cell body was heated until 200 °C, its center had still temperatures near 160 °C, when monitored continuously using a 1/16" end-welded thermocouple (not shown in Fig. 1) inserted through a 1/4" tube fitting-2. Two ZnSe windows-13 with an anti-reflective coating were used because of relatively high moisture contents during  $NH_3$ -SCR

reaction, and these window materials allowed high cell temperature and pressurized, if necessary, operations. Viton O-rings-14 (DuPont Performance Elastomers) were used to ensure high chemicals compatibility and good seals of the gas cell and placed in a groove on a window endplate-15 that was isolated by a ceramic insulating plate-16. An IR beam that has come out from its source is entered into the cell by an Au-coated plane transfer mirror-17 after passing through an inlet KBr window-18. After a trip in the gas cell according to defined pass numbers, the beam comes out through an outlet KBr window-19 to reach a detector. Details of the geometry of some components with this gas cell will be further discussed later.

#### 3-2. Gas Cell Geometry

The geometries of a White cell associated with gas flow patterns from point of input to output are very important to establish a fast exchange rate of gas samples and to prevent droplet nucleation of samples by adiabatic expansion in the cell. Although a variety of gas cell geometries are in use and serve as a good illustration of gas flow pattern characteristics, the cell geometry shown in Fig. 2 was used for this study, which is one of the most common cell designs for gas analysis applications. This geometry can give an uneven flow pattern of gas samples in the gas cell and lead to some dead spaces in a sample flow and very slow exchange rate of gas samples; however, these problems may be minor because very high total flow rates, by 1,000  $cm^3/min$  or more, of gas samples with an excellent homogeneity are used. Fig. 2(a) shows schematically the positions of the two objective mirrors-8 and single field mirror-11 and each corresponding geometry and of the K-type thermocouple to directly measure gas sample temperatures in the gas cell. The field mirror has corners on both sides that cut out to allow the IR beam to enter and exit the gas cell. The beam comes in the ZnSe window-13 on the right and reflects back and forth between the objective mirrors and the field ones, and after defined pass numbers it

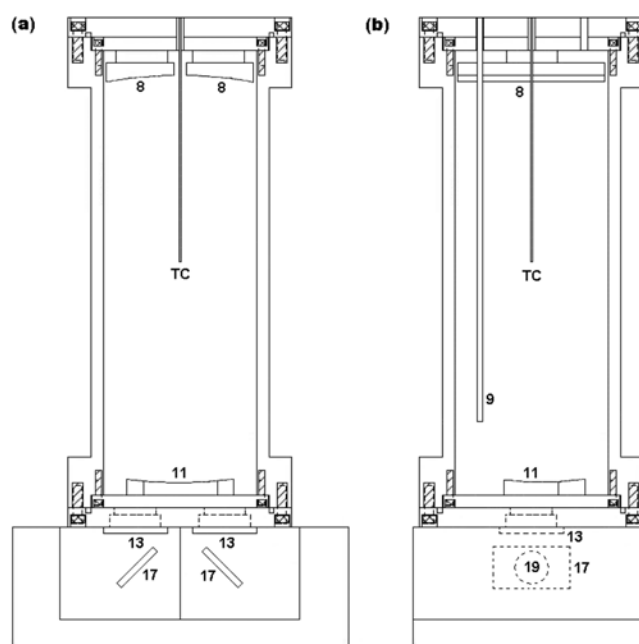


Fig. 2. White cell geometry in a front view of (a) a-a' and (b) b-b' in Fig. 1. The numbers are the same indication as those in Fig. 1.

exits through the left ZnSe window. The feedthrough-9 shown in Fig. 2(b) was of a 1/4" SS tube with a 26.7-cm length in the original gas cell.

### 3-3. Modifications of the White Cell

During our early studies of an on-line IR-based N<sub>2</sub>O measurement system with the commercially-available long pathlength White cell [21-23], we encountered significant reduction in the energy throughput after the use of the gas cell for a couple of months under our SCR conditions. This might result from physical contaminations and/or chemical damage of the surface of the mirrors. In a mixture consisting of NO<sub>x</sub>, NH<sub>3</sub>, and O<sub>2</sub> in a flow of pure He, the ammonia can react with NO<sub>2</sub> to form NH<sub>4</sub>NO<sub>3</sub> even at the cell inside temperature of 160 °C [24]. It can be deposited on the surface of the mirrors in the form of very thin film-like layers, accompanying such decrease in the net energy throughput after use for two to three months [21]. At temperatures near 170 °C, the solid-phase NH<sub>4</sub>NO<sub>3</sub> exists in equilibrium with NH<sub>3</sub> and HNO<sub>3</sub>, as the following stoichiometry [25,26]:



The vapor-phase HNO<sub>3</sub> can cause chemical damages of the surface of the mirrors in the gas cell.

Based on these possibilities regarding the physical contaminations and chemical alteration of the mirrors, it is important to circumvent the formation of NH<sub>4</sub>NO<sub>3</sub> under our feed gas conditions as well as to choose reflective coatings with stronger chemical compatibility. Therefore, a ZnSe coating on the surface of the double-layered Ni/Au-coated mirrors was subsequently allowed to improve the problems regarding the chemical resistance of the reflective coating materials to our feed gas conditions with a flowing mixture of NO<sub>x</sub>, NH<sub>3</sub>, and O<sub>2</sub>. To avoid the deposition of NH<sub>4</sub>NO<sub>3</sub> on the surface of the mirrors during usage of the gas cell under SCR conditions,

we needed to prevent its formation itself in the gas cell, and the old silicon-encapsulated heater was replaced to a BriskHeat *XtremeFLEX* BIH-G Series heating jacket capable of heating it to 260 °C, approaching to a cell center temperature of 210 °C at which NH<sub>4</sub>NO<sub>3</sub> completely decomposes [27] and no deposition of such NH<sub>4</sub><sup>+</sup> salts on the mirrors occurs. All the O-rings in the original gas cell were replaced with Kalrez 7075 O-rings (DuPont Performance Elastomers) that possess very strong thermal resistance.

When the original gas cell was employed for direct N<sub>2</sub>O measurements for NH<sub>3</sub>-SCR reaction, a response time approaching a steady state in N<sub>2</sub>O concentrations was very fast but not for NO<sub>x</sub> and NH<sub>3</sub>, which was due to the adsorption of NO<sub>x</sub> and NH<sub>3</sub> on the surface of the SS feedthrough tube-9 in Fig. 2(b). Therefore, it was substituted with a 1/4" quartz tube in our modified gas cell to minimize such an adsorption. Details of the mechanism of the reduction in the net energy throughput due to the formation of NH<sub>4</sub>NO<sub>3</sub> under SCR conditions are another program of this work in which spectroscopic observations of the contaminations and chemical alteration of the mirrors will be discussed [28].

### 4. System Configuration for Directly Measuring N<sub>2</sub>O from NH<sub>3</sub>-SCR Reaction

A "System A" consisting mainly of a feed gas handling system, homogenizer, continuous flow-type fixed-bed reactor, and pressure and temperature monitors has been constructed to simulate N<sub>2</sub>O emissions from many commercial NH<sub>3</sub>-SCR processes, as shown in Fig. 3. A homogenizer equipped with this reactor system was specially designed to facilitate complete mixing between feed gases, such as NO, NH<sub>3</sub>, O<sub>2</sub>, N<sub>2</sub>O, and SO<sub>2</sub>, in flowing He. A 180-mesh glass frit was inserted into the I-shaped Pyrex reactor with a 3/8" OD to keep fine powder samples. Pressures less than 3 psi (1 psi = 6.89 kPa) were indicated with this reactor system into which an appropriate amount of a fine powder sample of the commercial V<sub>2</sub>O<sub>5</sub>-

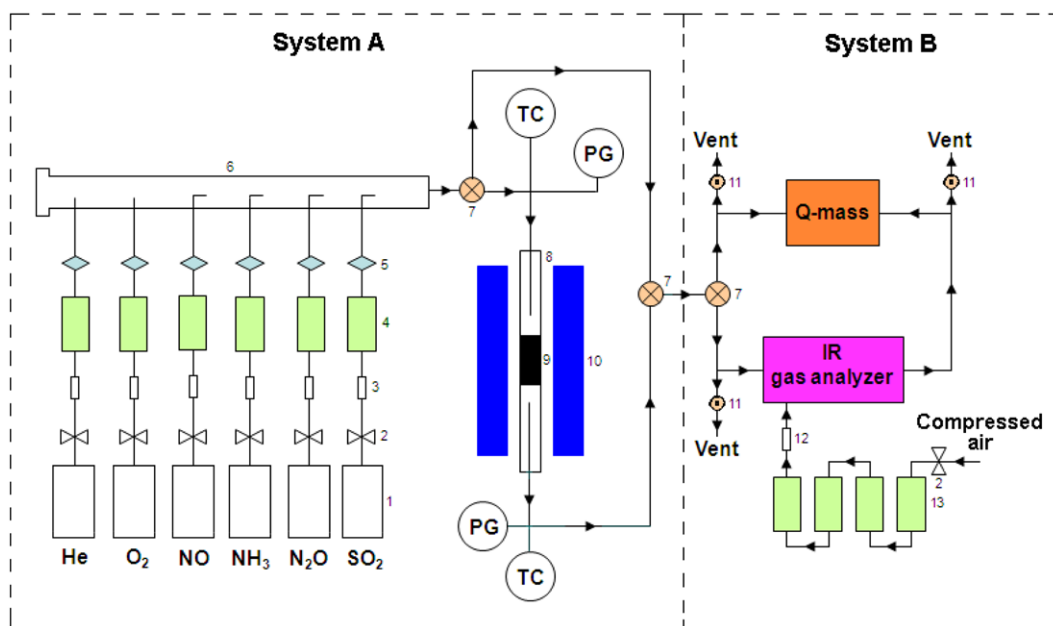


Fig. 3. Schematic of an on-line IR-based N<sub>2</sub>O measurement system combined with NH<sub>3</sub>-SCR DeNO<sub>x</sub> reactor: 1, gas cylinders; 2, on/off valves; 3, in-line filters; 4, mass flow controllers; 5, check valves; 6, mixing chamber; 7, 3-way valves; 8, I-shaped Pyrex reactor; 9, catalyst bed; 10, electric furnace; 11, micro-metering valves; 12, rotameter; 13, silica traps.

WO<sub>3</sub>/TiO<sub>2</sub> catalyst was charged. All SS lines and valves after the homogenizer were heated to 180 °C with a heating band to prevent homogeneous reaction between gases, particularly NO<sub>x</sub> and NH<sub>3</sub>. Details of this NH<sub>3</sub>-SCR reaction system have been provided elsewhere [22,23].

The System A was combined with a “System B” in Fig. 3 that is composed of the modified gas cell coupled with a computer-controlled Nicolet 7600 FT-IR spectrophotometer (Thermo Electron Corp.) with a theoretical resolution of 0.09 cm<sup>-1</sup> equipped with a liquid N<sub>2</sub>-cooled MCT-A detector and an HPR-20 QIC quadrupole mass spectrometer (Hidden Analytical Ltd.) to allow continuous monitoring and measurements for N<sub>2</sub>O production levels during the course of SCR reaction over the commercial TiO<sub>2</sub>-supported V<sub>2</sub>O<sub>5</sub> catalyst. This system configuration also allowed simultaneous estimates in NO<sub>x</sub> and NH<sub>3</sub> concentrations. During data collection, the entire FT-IR system was purged with a 15-L/min flow rate of a compressed air passed through a train of a laboratory-designed big silica trap for removing H<sub>2</sub>O in the air. Even after such a purification of the air, the airborne CO<sub>2</sub> and CO were still present and IR-active but did not disturb precise analysis for N<sub>2</sub>O, NO<sub>x</sub> and NH<sub>3</sub>, because of distinguishable peak positions that will be discussed below.

### 5. On-line Measurements of N<sub>2</sub>O Emissions from NH<sub>3</sub>-SCR Reaction

Direct measurements for N<sub>2</sub>O formation in NH<sub>3</sub>-SCR deNO<sub>x</sub> reaction at given reaction temperatures were conducted using the on-line, computer-controlled IR analysis system. A sample of the 1.68% V<sub>2</sub>O<sub>5</sub>-7.6% WO<sub>3</sub>/TiO<sub>2</sub> catalyst (*ca.* 0.5 g) was loaded into the I-shaped Pyrex reactor placed in a Lindberg Model HTF55347C split-hinge tube furnace with a three-independent heating zone in the System A shown in Fig. 3, and an He flow with 21% O<sub>2</sub> (Praxair, 99.999%) at a total flow rate of 1,000 cm<sup>3</sup>/min, corresponding to a gas hourly space velocity (GHSV) of 76,200 h<sup>-1</sup>, passed through this reactor to allow *in situ* sample calcinations at 500 °C for 1 h. Under this flowing mixture, the reactor with the catalyst was cooled to 200 °C at which the System A was purged with pure He at the same flow rate for 30 min, and this pure He was flowed through the gas cell in the System B to fully purge it at the cell inner temperature of 210 °C for 1 h. Then, the gas flow was scanned at 210 °C to obtain an interferogram which was employed as a background for Fourier transforming gas-phase spectra for gas samples obtained during NH<sub>3</sub>-SCR reaction under given conditions. Following this, a typical gas mixture of 500 ppm NO<sub>x</sub>, 500 ppm NH<sub>3</sub> and 5% O<sub>2</sub> in He at the total flow rate detoured the reactor with the catalyst bed and was passed through the gas cell for 30 min. A second interferogram was taken under this upstream gas flow and it was used as a reference spectrum to quantify the extent of N<sub>2</sub>O formation and NO<sub>x</sub> and NH<sub>3</sub> consumptions in NH<sub>3</sub>-SCR deNO<sub>x</sub> reaction, the flowing mixture was directed to the catalyst bed to conduct the reaction as a function temperature, and then final interferograms were collected during this SCR reaction. All interferograms were recorded with a resolution of 0.5 cm<sup>-1</sup> and a scan number of 100. Temperatures of the Pyrex reactor during each experimental run were monitored by using a K-type thermocouple that had been inserted into the reactor and positioned just above the catalyst bed. They were controlled by using a three-independent microprocessors-based PID controller (Lindberg, Model CC584343PC). The He used was further purified by passing it through a moisture trap (Alltech Assoc.). All gas

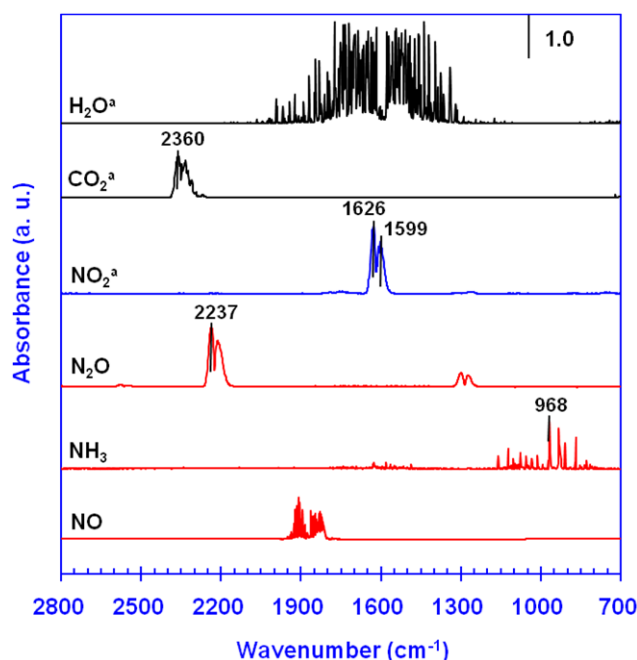


Fig. 4. IR spectra for 100 ppm NO, 100 ppm NH<sub>3</sub>, and 100 ppm N<sub>2</sub>O in a flow of pure He. “Spectra for 100 ppm NO<sub>2</sub>, 1,500 ppm CO<sub>2</sub>, and 1,000 ppm H<sub>2</sub>O in a flow of either air or N<sub>2</sub> at 25 °C and 14.7 psi were obtained from a Thermo Spectral QC Library.

flows were accurately controlled using Brooks 5850E and Bronkhorst F-200CV mass flow controllers.

## RESULTS AND DISCUSSION

Not only should NO<sub>2</sub> and H<sub>2</sub>O be produced during the course of NO-NH<sub>3</sub>-O<sub>2</sub> reaction with the commercial V<sub>2</sub>O<sub>5</sub>-WO<sub>3</sub>/TiO<sub>2</sub> catalyst [24,26], but CO<sub>2</sub> is also present in the background interferogram as stated already. Therefore, gas-phase spectra for N<sub>2</sub>O, NH<sub>3</sub>, and NO with a 100-ppm concentration in a flow of pure He were compared with those of H<sub>2</sub>O, NO<sub>2</sub> and CO<sub>2</sub> chosen in a Thermo Spectral QC Library. This procedure can allow us to distinguish accurate position of reference peaks in sample spectra later. All spectra are given in Fig. 4. The spectrum of N<sub>2</sub>O in the flowing mixture had the most intense peak at 2,237 cm<sup>-1</sup> with a peak at 2,212 cm<sup>-1</sup>, and these peaks are distinctive with those in the gas-phase spectrum of CO<sub>2</sub> that gives a strong band at 2,360 cm<sup>-1</sup>. A peak at 968 cm<sup>-1</sup> for NH<sub>3</sub> appeared with substantial peaks at 932 and 868 cm<sup>-1</sup>. These results are in very good agreement with the previous works [29,30]. Peaks at 1,626 and 1,599 cm<sup>-1</sup> in the spectrum for NO<sub>2</sub>, which can be produced under SCR conditions, particularly in the presence of O<sub>2</sub>, are observed, and the 1,599 cm<sup>-1</sup> band is distinguishable with all peaks existing in gas-phase H<sub>2</sub>O spectrum. However, the pure NO possessed complicated peaks at 1,950 to 1,800 cm<sup>-1</sup> and some peaks were overlapped with those appeared at the high frequency side of the H<sub>2</sub>O spectrum.

Spectrum for 100 ppm NO in a flowing He with ambient air, that contains a small amount of H<sub>2</sub>O vapor depending on the air temperatures, was collected to differentiate NO and H<sub>2</sub>O peaks and to choose only a single reference peak among the complicated NO bands at

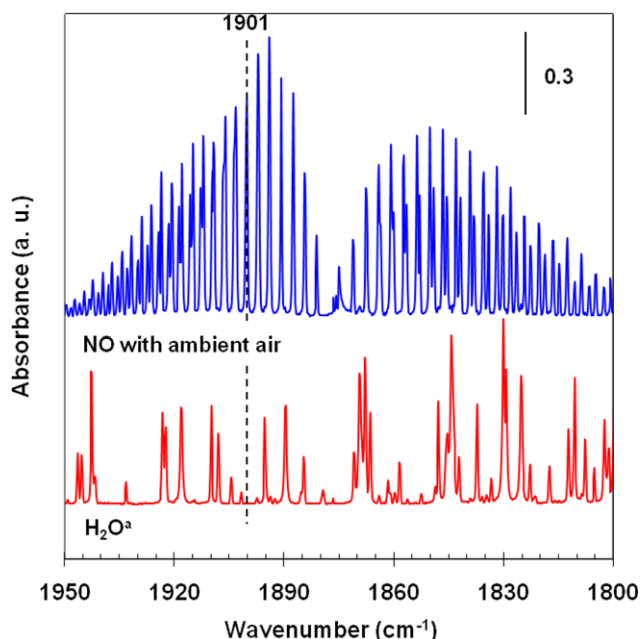


Fig. 5. Differentiation between gas-phase NO and H<sub>2</sub>O IR peaks at 1,950-1,800 cm<sup>-1</sup>. The NO was diluted in ambient air. "Spectrum for 1,000 ppm H<sub>2</sub>O in a flow of N<sub>2</sub> at 25 °C and 14.7 psi was obtained from a Thermo Spectral QC Library.

wavenumbers from 1,950 to 1,800 cm<sup>-1</sup>. NO peaks at this frequency region were compared with those in the H<sub>2</sub>O-only spectrum, as shown in Fig. 5. Many of the peaks for NO were coincident with those indicated for gas-phase H<sub>2</sub>O alone; however, a peak at 1,901 cm<sup>-1</sup> had only a single position and this was chosen as a reference peak of NO to monitor variations in its gas-phase concentrations during NH<sub>3</sub>-SCR deNO<sub>x</sub> reaction later. Consequently, the 2,237, 1,901, 1,599 and 968 cm<sup>-1</sup> bands were used as the respective reference peaks for N<sub>2</sub>O, NO, NO<sub>2</sub> and NH<sub>3</sub>, when calibrating the modified White cell combined with the IR spectrometer as a function of each gas concentration and determining changes in NO<sub>x</sub> and NH<sub>3</sub> concentrations during the course of catalytic deNO<sub>x</sub> reaction at given reaction temperatures.

The on-line IR-based N<sub>2</sub>O measurement system was calibrated at an IR beam pathlength of 8.0 m and a cell center temperature of 210 °C using a flowing mixture consisting of 0-240 ppm N<sub>2</sub>O in He. All collected data up to concentrations near 240 ppm would be lined up on a third-order polynomial (not shown here) and this equation was transposed to our software setups to determine N<sub>2</sub>O concentrations from NH<sub>3</sub>-SCR reaction with the commercial V<sub>2</sub>O<sub>5</sub>-WO<sub>3</sub>/TiO<sub>2</sub> catalyst. Substantial presence of 5% O<sub>2</sub> in the N<sub>2</sub>O/He flowing mixture gave no change in N<sub>2</sub>O concentrations tested, as expected. The gas handling system allowed NO and NH<sub>3</sub> to be flowed through the gas cell as a flowing mixture in He to obtain similarly a calibration curve for each gas that was used for determining NO<sub>x</sub> and NH<sub>3</sub> conversions during SCR reaction later.

Spectra for 5 ppm N<sub>2</sub>O in an He flowing mixture were obtained with respect to the pathlength of IR beam in the White cell, as provided in Fig. 6. When the beam pathlength increased, a main peak at 2,237 cm<sup>-1</sup> with a weaker one at 2,212 cm<sup>-1</sup> became more intense, which is associated with increased IR signals even for the same moles

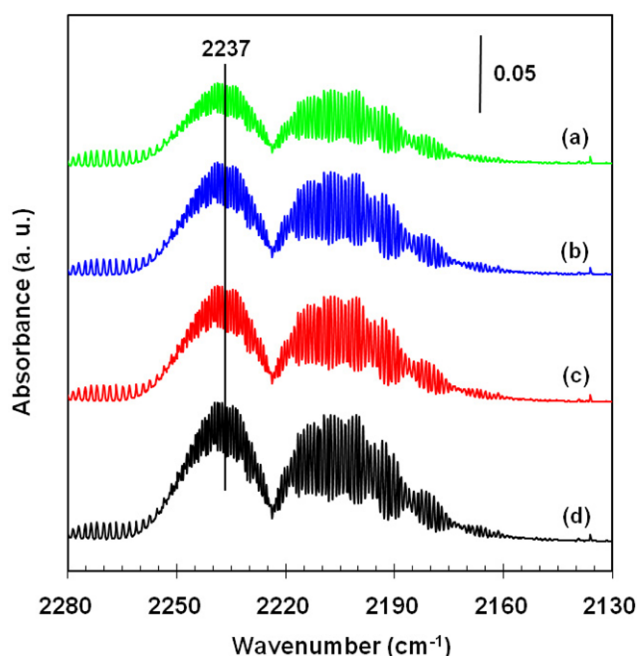


Fig. 6. Gas-phase IR spectra for 5 ppm N<sub>2</sub>O in a flow of pure He as a function of a beam pathlength: (a) 4.0; (b) 5.6; (c) 6.4; (d) 8.0 m.

of N<sub>2</sub>O in the gas cell [31]. This implies that we would detect smaller N<sub>2</sub>O amounts as the pathlength increases. In theory, the extent of the energy throughput decreases when the pathlength of IR beam becomes long. However, the longer the pathlength, at a given concentration the more gas molecules are counted by the IR beam [31, 32] and we will gain more intense signals in infrared absorption, although there is the competing process of creating more noise levels because the IR signals are reduced due to mirror reflection and scattering losses. Keeping this principle in mind, we need to consider the following aspects prior to determining the best number of reflections, *i.e.*, the pathlength of the IR beam. First, our gas cell coupled with IR spectroscopy is normally operated at a continuous flow of gas samples, although it was designed so as to be worked both at high pressures up to 45 psi and in vacuum as described previously. Secondly, the concentration of N<sub>2</sub>O emitted from fossil fuels-fired power plants was less than 5 ppm [18-20] and independent of the kinds of fossil fuels being used, as stated already. Based on these points regarding our continuous N<sub>2</sub>O measurements using the combined White cell-IR system, the pathlength is desirable to be set to 8.0 m to determine if conventional NH<sub>3</sub>-SCR processes play a significant role in creating substantial N<sub>2</sub>O formation.

The selective NO<sub>x</sub> reduction with NH<sub>3</sub> over 1.68% V<sub>2</sub>O<sub>5</sub>-7.6% WO<sub>3</sub>/TiO<sub>2</sub> as a representative commercial SCR catalyst was conducted at the System A as a function of reaction temperature, and all spectra of the resulting gases were collected at the pathlength of 8.0 m using the System B; selected gas-phase IR spectra are shown in Fig. 7. At 2,237 cm<sup>-1</sup>, there was no appreciable N<sub>2</sub>O peak even with the catalyst at temperatures until 350 °C (not included here), but at higher temperatures the peak is clearly visible. The intensities of characteristic peaks for NH<sub>3</sub> with the most intense one at 968 cm<sup>-1</sup> decreased with exposure of the NO<sub>x</sub>-NH<sub>3</sub>-O<sub>2</sub> flow to the cata-

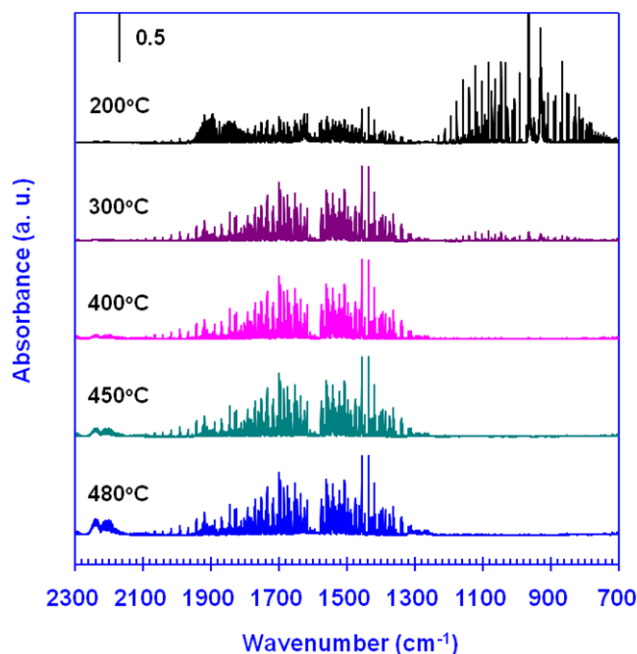


Fig. 7. Gas-phase IR spectra of gas samples during  $\text{NH}_3$ -SCR reaction over a commercial  $\text{V}_2\text{O}_5$ - $\text{WO}_3/\text{TiO}_2$  catalyst as a function of reaction temperature. All spectra were collected at a 8.0-m beam pathlength of the gas cell.

lyst at 200 to 480 °C, as expected, and the reference peak of  $\text{NO}$  was also lowered during this reaction. On the other hand, the bands by  $\text{H}_2\text{O}$  increased up to 400 °C, which is related to the production of  $\text{H}_2\text{O}$  from this SCR reaction. This represents that a typical SCR reaction between  $\text{NO}_x$  and  $\text{NH}_3$  in the presence of  $\text{O}_2$  occurs, and during that catalytic reaction  $\text{N}_2\text{O}$  is formed, depending on reaction temperatures.

When putting the intensity data of each reference peak for  $\text{N}_2\text{O}$ ,  $\text{NO}_x$  and  $\text{NH}_3$  in the spectra obtained during the  $\text{NH}_3$ -SCR reaction

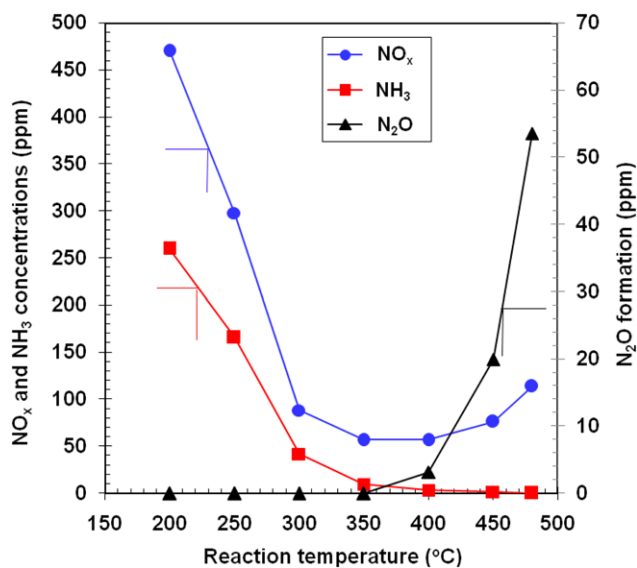


Fig. 8.  $\text{N}_2\text{O}$  concentrations produced during  $\text{NH}_3$ -SCR reaction over a commercial  $\text{V}_2\text{O}_5$ - $\text{WO}_3/\text{TiO}_2$  catalyst.

into our software setup protocols for quantifications, this commercial catalyst showed significant amounts of  $\text{N}_2\text{O}$  production, ca. 20 and 55 ppm at the respective temperatures of 450 and 480 °C, although the  $\text{N}_2\text{O}$  formation is not probable at temperatures less than 400 °C, as seen in Fig. 8, and the 55 ppm  $\text{N}_2\text{O}$  is equivalent to 1.7%  $\text{CO}_2$  emissions, based on the GWP value for  $\text{N}_2\text{O}$ . The catalyst gave a decrease in both  $\text{NO}_x$  and  $\text{NH}_3$  concentrations as reaction temperature increased to 400 °C, but greater ones  $\text{NO}_x$  concentrations increased apparently. This behavior in the  $\text{NO}_x$  concentration at high temperatures is due to the competing mechanism of oxidizing  $\text{NH}_3$ , because of relatively high activation energy of its oxidation reaction [33]. At the active window ranging 300 to 450 °C, the observed  $\text{NO}_x$  concentrations corresponded to catalytic activities greater than 90%  $\text{NO}_x$  conversion, although this catalyst had conversions less than 60% at temperatures lower than 300 °C. Consequently, it is clear that the  $\text{deNO}_x$  reaction under our SCR conditions substantially produced  $\text{N}_2\text{O}$  with significant levels as the following reaction:



This is consistent with an earlier study of  $\text{NH}_3$ -SCR reaction over 3%  $\text{V}_2\text{O}_5$ -9%  $\text{WO}_3/\text{TiO}_2$  that revealed 20-180 ppm  $\text{N}_2\text{O}$  at temperatures ranging from 350 to 475 °C [34].

## CONCLUSIONS

A combination of a commercially available IR spectrometer and a variable long path White gas cell has been used to develop an on-line analysis system for directly determining  $\text{N}_2\text{O}$  emission levels in  $\text{NH}_3$ -SCR reaction with no artifact errors reported in the literature. The problems acquired from our earlier studies require modifications of the gas cell to improve the chemical compatibility to  $\text{NH}_3$ -SCR conditions and the possible damage of the surface of the mirrors. This on-line IR analysis system coupled with our modified gas cell may be very useful for measuring actual levels in  $\text{N}_2\text{O}$  emissions from fossil fuel-fired power plants with commercial  $\text{NH}_3$ -SCR  $\text{deNO}_x$  processes. As a model case of  $\text{deNO}_x$  industries for such utility facilities, we studied direct  $\text{N}_2\text{O}$  measurements for  $\text{NH}_3$ -SCR reaction over a commercial  $\text{V}_2\text{O}_5$ - $\text{WO}_3/\text{TiO}_2$  catalyst. Gas-phase spectra for  $\text{N}_2\text{O}$ ,  $\text{NO}_x$  and  $\text{NH}_3$  including possible interferences are collected and resolved to choose each reference peak; conditions for a continuous operation of the system are optimized in order to obtain good spectra for  $\text{N}_2\text{O}$  even with very low concentrations. The system allows a real time monitoring in the formation of  $\text{N}_2\text{O}$  during the course of the reaction, and it gives simultaneous determination of  $\text{NO}_x$  and  $\text{NH}_3$  concentrations as a function of on-stream time and reaction temperature. There was significance in the extent of the  $\text{N}_2\text{O}$  production during the SCR reaction, depending strongly on given reaction temperatures.

## ACKNOWLEDGEMENT

This study was supported by a partial grant-in-aid via ETEP Grant # R-2007-1-002-0.

## REFERENCES

1. C. Kroeze, *Sci. Total Environ.*, **152**, 189 (1994).

2. G. Centi, S. Perathoner and F. Vazzana, *Chemtech*, **29**, 48 (1999).
3. J. Perez-Ramirez, F. Kapteijn and A. Bruckner, *J. Catal.*, **218**, 234 (2003).
4. K. Doi, Y. Y. Wu, R. Takeda, A. Matsunami, N. Arai, T. Tagawa and S. Goto, *Appl. Catal. B*, **35**, 43 (2001).
5. B. Leckner and A. Lyngfelt, *Int. J. Energy Res.*, **26**, 1191 (2002).
6. L. Lietti, I. Nova, G. Ramis, L. D. Acqua, G. Busca, E. Giamello, P. Forzatti and F. Bregani, *J. Catal.*, **187**, 419 (1999).
7. G. Madia, M. Elsener, M. Koebel, F. Raimondi and A. Wokaun, *Appl. Catal. B*, **39**, 181 (2002).
8. J. A. Martin, M. Yates, P. Avila, S. Suarez and J. Blanco, *Appl. Catal. B*, **70**, 330 (2007).
9. M. Yates, J. A. Martin, M. A. Martin-Luengo, S. Suarez and J. Blanco, *Catal. Today*, **107/108**, 120 (2005).
10. S. Suarez, J. A. Martin, M. Yates, P. Avila and J. Blanco, *J. Catal.*, **229**, 227 (2005).
11. L. Lietti, I. Nova and P. Forzatti, *Top. Catal.*, **11/12**, 111 (2000).
12. L. Singoredjo, R. Korver, F. Kapteijn and J. Moulijn, *Appl. Catal. B*, **1**, 297 (1992).
13. H. Sjøvall, L. Olsson, E. Fridell and R. J. Blint, *Appl. Catal. B*, **64**, 180 (2006).
14. W. M. Hao, S. C. Wofsy, M. B. McElroy, J. M. Beer and M. A. Toqan, *J. Geophys. Res.*, **92**, 3098 (1987).
15. J. C. Kramlich, J. A. Cole, J. M. McCarthy, W. S. Lanier and J. A. McSorley, *Combust. Flame*, **77**, 375 (1989).
16. L. J. Muzio and J. C. Kramlich, *Geophys. Res. Lett.*, **15**, 1369 (1988).
17. L. J. Muzio, M. E. Teague, J. C. Kramlich, J. A. Cole, J. M. McCarthy and R. K. Lyon, *J. Air Pollut. Control Assoc.*, **39**, 287 (1989).
18. T. Hulgaard and K. Dam-Johansen, *Environ. Progr.*, **11**, 302 (1992).
19. W. P. Linak, J. A. McSorley, R. E. Hall, J. V. Ryan, R. Srivastava, J. O. L. Wendt and J. B. Mereb, *J. Geophys. Res.*, **95**, 7533 (1990).
20. M. J. F. Gutierrez, D. Baxter, C. Hunter and K. Svoboda, *Waste Manage. Res.*, **23**, 133 (2005).
21. Y. H. Lee and M. H. Kim, Unpublished results.
22. K. H. Kim, Y. H. Lee, M. H. Kim, S. W. Ham, S. M. Lee and J. B. Lee, in Proceedings of 5<sup>th</sup> International Conference on Environmental Catalysis, Belfast, Aug. 31-Sep. 3, 2008, Paper # 450.
23. Y. H. Lee, M. H. Kim and S. W. Ham, in Proceedings of 21<sup>st</sup> North American Catalysis Society Meeting, San Francisco, CA, June 7-12, 2009, Paper # P-M-143.
24. I. Nova, C. Ciardelli, E. Tronconi, D. Chatterjee and M. Weibel, *Top. Catal.*, **42/43**, 43 (2007).
25. A. W. Stelson and J. H. Seinfeld, *Atmos. Environ.*, **16**, 983 (1982).
26. M. Koebel, G. Madia and M. Elsener, *Catal. Today*, **73**, 239 (2002).
27. G. Feick and R. M. Hainer, *J. Am. Chem. Soc.*, **76**, 5860 (1954).
28. Y. H. Lee, M. H. Kim and S. W. Ham, *Appl. Spectrosc.*, Submitted (2010).
29. L. Rosenmann, B. Khalil and R. Le Doucen, *J. Quant. Spectrosc. Radiat. Transfer*, **57**, 477 (1997).
30. D. W. T. Griffith and B. Galle, *Atmos. Environ.*, **34**, 1087 (2000).
31. B. R. Stallard, L. H. Espinoza, R. K. Rowe, M. J. Garcia and T. M. Niemczyk, *J. Electrochem. Soc.*, **142**, 2777 (1995).
32. J. U. White, *J. Opt. Soc. Am.*, **32**, 285 (1942).
33. I. Nova, C. Ciardelli, E. Tronconi, D. Chatterjee and B. Bandl-Konrad, *AIChE J.*, **52**, 3222 (2006).
34. S. Djerad, M. Crocoll, S. Kureti, L. Tifouti and W. Weisweiler, *Catal. Today*, **113**, 208 (2006).